Estimating Soybean Yield Spatial Variability Within-field Scale through Google Earth Engine in Northeast Italy

Alessandro Zanchin*, Marco Sozzi, Francesco Marinello, Ahmed Kayad

Department TESAF, University of Padova, Legnaro (PD), Italy

* Corresponding author. Email: alessandro.zanchin@phd.unipd.it

Abstract

The study of spatial variability within agricultural fields is essential for all farmers who want to apply modern precision agriculture. This study investigated the possibility of estimating soybean yield spatial variability at field scale through different vegetation indices (VIs) derived from Sentinel-2 satellite images at different crop growth stages. The study considered yield records from seven fields located in North-East of Italy, with areas ranging between 10 to 19 ha and cultivated by soybean from 2016 to 2018. Sentinel-2 satellite images were used to calculate eight VIs through Google Earth Engine (GEE) between June to October. One-way ANOVA tested the linear correlation between yield and VIs measured at different soybean phenological stages corresponding to the available cloud-free Sentinel-2 images. Results showed that Green Chlorophyll Vegetation Index (GCVI), Green Normalized Difference Vegetation Index (GNDVI) and Wide Dynamic Range Vegetation Index (WDRVI) were the best correlated VIs with soybean yield variability. The highest correlation was observed between 85 and 105 days after sowing corresponding to grains forming and filling (phenological stage R4-R6). R^2 values ranged between 0.21 and 0.68 across whole fields and growth stages. The study proved the effectiveness of a linear model exploiting the equation of the regression line between the VIs and soybean yield from the field with the highest correlation. The model showed high yield estimation accuracy results in 2018 and 2017 seasons with root mean square error (RMSE) of 0.47 and 0.49 Mg/ha respectively compared to less accuracy in 2016 where RMSE was 1.02 Mg/ha. This study approach proved the ability to estimate the within-field variability of soybean yield which could be applied to other Sentinel-2 archived images starting from 2015, while a new model should be calculated each year for each geographic region to ensure the estimation accuracy.

Keywords: Remote sensing, within-field variability, Sentinel-2, soybean.

1. Introduction

Yield maps provide a representation of the crop response to spatial patterns from soil features and topography and temporal patterns as weather conditions or pests and diseases spreading. The recent availability of low-cost (Srbinovska et al. 2015) and freely available high-resolution images from satellites (Sishodia et al., 2020) increased all that helpful data to explain the within-field variability of agricultural areas. All this information is a key factor for all farmers and technicians who target the proper agricultural management of their fields according to precision agriculture (PA). Moreover, the accurate estimation can provide information for insurances and market decision purpose (Lobell 2013). PA is an integrated way of farming to improve the efficiency of agricultural resources through minimising the uncertainty of fields variability management (Liaghat and Balasundram 2010). PA can increase yield and reduce environmental impact and input costs through the site-specific management of homogenous zones (Basso et al. 2016; Kayad et al. 2021). Considering the aforementioned concepts, PA is one of the farming methods with the lowest environmental impact per food unit, ensuring the healthiness of goods simultaneously (Tellaeche et al. 2008). Variable-rate technology (VRT) is an example of precision agriculture tools to manage the within-field variability. VRT allows changing the spreading rate of agricultural inputs and soil tillage according to prescription maps. Monitoring variables of interest lead to estimate the within-field variability and subsequently the required application rate according to crop needs (Leroux and Tisseyre 2019). A common way for monitoring fields and crops is remote sensing (RS). RS is a science, technology, and art that allows the detection and analysis of objects on the earth's surface and below, without any physical contact between the sensor, the operator who collects data, and the targets (Thomas et al., 2015). Satellites are available to monitor agricultural areas for decades (Sishodia et al., 2020). For agricultural applications, the bands within the visible and near-infrared (NIR) reflectance from the crops play a crucial role in crops monitoring. The study of the NIR region allows detecting crop vigour, stress and health issues (Thomas et al.,1997). The reflection of NIR frequencies changes according to the chemical composition of the vegetal tissues, for examples, different plant species, different crops phenological stage and plant health (Foley et al. 1998). Many vegetation indices (VIs) have been proposed to monitor crops, forests and natural areas (Xue and Su 2017). VIs represent a powerful tool to monitor and assess crop variability (Bolton and Friedl 2013). VIs means a mathematical function between the absorbance value of specific frequencies of light reflected by the canopy of both crops and plants and catches by an optical sensor. The ratio between the quantity of

light absorbed by the chlorophyll and other pigments with the light reflected by vegetal tissues is directly related to plants biomass and health status (Zhang et al. 2012). VIs clearly portray these crops features. Normalized vegetation index (NDVI) was proposed by Rouse et al., in 1973, and it retrieves the concentration of chlorophyll expressed from 0 to 1 on plant tissues. It is considered a base method to detect vigour plants rich in chlorophyll than weak plants. Many other VIs was proposed for several purposes. EVI is an example of formula built by Liu and Huete to improve NIR detection avoiding atmospheric interferences. Soil-Adjusted Vegetation Index (SAVI) separates the soil background noise from the light reflected by the crop canopies (Huete 1988). Gitelson designed the Wide Dynamic Range Vegetation Index (WDRVI) that is more sensitive at high chlorophyll concentration while NDVI easily reaches saturation (Xue and Su 2017). Each change on plants tissues has a different effect on the reflected light spectrum (Mahlein et al. 2013). Many indexes were proposed to identify different causes of stress according to the changes in the spectrum of emitted light by the crops. Many authors studied the spatial distribution of stress correlation with the trend of VIs in the same field. If this correlation is significant, it means that VIs is suitable to assess and monitor the spreading of a stress factor (Oumar and Mutanga 2013). As mentioned above, VIs let to detect nutrient deficit and identify in which area of the field they are much required (Basso et al. 2016). Health status monitoring (Xue and Su 2017) and yield estimation (Schwalbert et al. 2018) are some examples of the power of RS for crops monitoring. exploiting VIs. Many studies proved the effectiveness of using Sentinel-2 images to compute VIs and then estimate yield and within-field crop variability (Hunt et al. 2019). Sentinel-2 represents two satellites of the mission Copernicus Sentinel-2 launched by the European Space Agency (ESA). First images of the earth surface have been available since June 2015. Sentinel-2 mount a multispectral sensor. Four bands have a spatial resolution of 10m, six 20m and three 60m and the revisit time is five days at the equator. All data are freely available through ESA and Google earth engine (GEE) platforms. Comparing yield maps with VIs maps from satellite images is a proven method to explore the availability of detecting within-field variability of agricultural areas from RS (Schwalbert et al. 2018; Bolton and Friedl 2013; Al-Gaadi et al. 2016). Schwalbert et al., used NDVI maps from Sentinel-2 to estimate corn yield with a forecast model. This study retrived better results at farm scale than larger areas. Bolton et al., estimated corn and soybean variability at country-level in the Unites states thanks to MODIS (Moderate Resolution Imaging Spectroradiometer), a satellite owned by NASA (National Aeronautics and Space Administration). In this case, Enhanced Vegetation Index (EVI) fit better with their forecasting models than NDVI. Al-Gaadi et al., explored potato yield variability in Saudi Arabia at field-level comparing two satellite, Landsat-8 and Sentinel-2, and two VIs, NDVI and SAVI. Kayad et al., focused their research on the study of within-field variability of corn in the North Italy comparing many VIs from several Sentinel-2 images. Green Normalized Difference Vegetation Index (GNDVI) provided the highest correlation with corn yield variability. However, more investigations from real farms data, different field crops, different crop growth stages and at the field scale are needed.

Therefore, this study focused on the correlation analysis between VIs and the yield of soybean crop. The main objectives were to

1. Identify VIs that better estimates soybean yield spatial variability within field scale.
2. Verify in which phenological stage the correlation between VIs and soybean yield is higher.

2. Materials and Methods

2.1. Study area

This study considered seven fields located in the Veneto region in North-East of Italy, in the province of Rovigo, figure 1. These fields are located in an alluvial plain, and they have a clayey soil texture. The nearby distance between the seven study fields minimizes soil features and crop difference. In addition, the nearby distance helps to avoid any errors in monitoring due to the different incidence angle between the reflected light and the satellite position. The chosen fields have areas higher than 10ha, and they have a regular and polygonal shape. The same farmer cultivated these areas with soybean in 2016, 2017, and 2018 according to conventional management practices. He sowed soybean only once in three years per field, so no repetitions were available for the same field. Soybean is a summer crop (Legumes in Cropping Systems), and Italian farmers usually cultivate soybean from April to October. The seven field features are summarized in table 1.

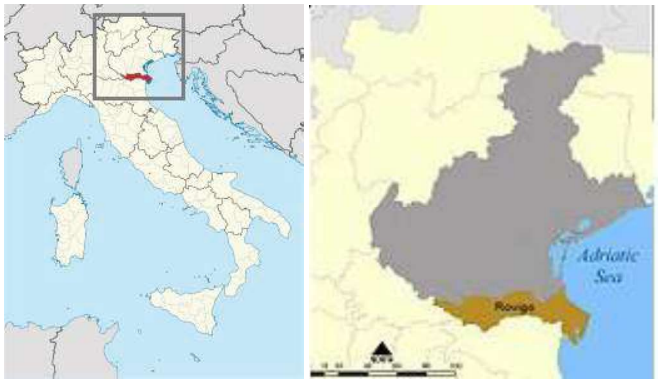

Figure 1. Study area, where the 7 fields considered as case studies were localized.

Table 1. Features of the seven areas considered for this study.

Field Name	Area (ha)	Crop	Sowing Date	Harvest Date	Average Yield (Mg/ha)
CNS	18.4	Soybean	May 20, 2018	Sept 18, 2018	4.15
RFS	12.5	Soybean	May 20, 2018	Sept 18, 2018	3.75
PVS	10.8	Soybean	May 12, 2017	Sept 17, 2017	3.42
AFS	9.4	Soybean	May 11, 2017	Sept 23, 2017	3.06
PAS	11.4	Soybean	Apr 25, 2017	Sept 21, 2017	3.05
RZS	15.1	Soybean	May 15, 2016	Sept 16, 2016	4.31
BDS	10.5	Soybean	May 8, 2016	Sept 13, 2016	4.74

2.2. Yield data

Yield records and maps were provided by Mantovani Lino & Loris agricultural companies. The farmer harvested each field with the same combine "Case IH AXIAL-FLOW 9230", thanks to the "AFS Harvest Command™" technology, that retrieved yield maps from its monitor "AFS Pro 700". Considering that the system records yield data per second, and the harvester works at 7 km/h mounting a header of nine meters wide, the monitor recorded at least 570 data points per hectare. SMS basic (AgLeader) is the software that lets to download the yield maps from the combine monitor. Raw yield maps have been cleaned from non-representative data in ArcMap10.3.1 (Esri), excluding all points less than 10m from the field border, and deleting all data further than three standard deviations from each field yield mean (Amidan et al., 2005; Córdoba et al. 2016). Yield records weredata interpolated in ArcMap10.3.1 with the kriging function to generate a continuous raster instead of a point data. Finally, the maps were resampled to match with the exact resolution of the satellite maps. All available yield maps were treated with the same procedure mentioned above.

2.3. Satellite monitoring

The monitoring started from the first week of June corresponding to 20 to 40 days after sowing (DAS) depending on the sowing date, and ended at soybean harvest. Sentinel-2 Level 2A (L2A) images were available on Google Earth Engine (GEE). GEE is a free Google LLC service available on the cloud, and it provides images from many satellite missions. It lets many transformations and computations on maps and satellite images and download the elaborated products. For this study, the bands one, three, four, five, and eight (Table 2) corresponding to blue, green, red, red-edge and near-infrared bands were used to compute eight VIs from Sentinel-2 images (Table 3). The eight VIs chosen for this research was the most common found in the literature review. For this study EVI formula was modify to obtain values from -1 to +1 adding a factor as showed in equation (1). Satellite images from June to October were suitable to monitor soybean during each developing growth stage. GEE filtered all pictures with more than 20% of the pixel covered by clouds. Summer is the best period of the year to monitor crops exploiting remote sensing because of the high number of available images in low cloudy cover; nevertheless, only a foggy day could affect the study results. GEE provided a raster with the same border of the field including the eight VIs values computed in each data when images were available and resampled at 10m pixel, the lowest available resolution from Sentinel-2 bands.

$$\mathrm{EVI} = \frac{\mathrm{B8} - \mathrm{B4}}{\mathrm{B8} + 6\mathrm{B4} - 7{,}5\mathrm{B1} + 10000} \quad (1)$$

Table 2. Sentinel-2 bands features, from www.sentinels.copernicus.eu.

Sentinel-2 Bands	Central Wavelength (nm)	Spatial resolution
B1 – Coastal Aerosol	443	60
B3 – Green	560	10
B4 – Red	665	10
B5 – Vegetation Red Edge	705	20
B8 - NIR	842	10

Table 3. Acronym, full name, equation and references of all vegetation indexes used in this research.

Acronym	Full name	Formula	Reference
NDVI	Normalized difference vegetation index	$(B8 - B4)/(B8 + B4)$	(Rouse et al., 1973)
NDRE	Normalized Difference Red Edge	$(B8 - B5)/(B8 + B5)$	(Barnes et al. 2000)
GNDVI	Green Normalized Difference Vegetation Index	$(B8 - B3)/(B8 + B3)$	(Gitelson et al., 1996)
GARVI	Green Atmospherycally Resistant Vegetation Index	$\frac{B8 - (B3 - B1 - B5)}{B8 - (B3 + B1 - B5)}$	(Gitelson et al., 1996)
EVI	Enhance Vegetation Index	$(B8 - B4)/(B8 + 6B4 - 7{,}5B1 + 1)$	(Liu and Huete 2019)
WDRVI	Wide Dynamic Range Vegetation Index	$(\alpha * B8 - B4)/(\alpha * B8 + B4)$	(Gitelson 2004)
GCVI	Green Chlorophyll Vegetation Index	(B8/B3)-1	(Gitelson et al., 2003)
mWDRVI	Wide Dynamic Range Vegetation Index	$\begin{cases} NDVI & NDVI \leq 0.6 \\ WDRVI & NDVI > 0.6 \end{cases}$	(Sakamoto et al., 2013)

2.4. Data analysis

Each yield map of the seven fields has been compared with its eight VIs rasters per all available dates. Each pairing was used for determining the correlation between yield and the VIs spatial trend by computing the R-squared value (R^2) and the regression line equation. Finally, ANOVA tested the significance of correlations between the two variables. The acquisition date of satellite images was expressed in days after the crop sowing (DAS) to compare the three different years. A time-series analysis let to understand which was the best VIs and when the correlation between yield and VIs was higher. The time-series also showed the field with the highest correlation. Once determined the field and the date with the highest R^2 values, the regression line between the most correlated VIs with soybean yield variability was chosen as a linear model to estimate the yield variability in the other six fields, by applying the model on the VIs map. The estimated yield was compared with the actual yield to test the accuracy of the model. Hence the Root Mean Square Error (RMSE), equation (2) and the correlation between estimated and actual yield proved the effectiveness of the estimation thanks to the linear model.

$$RMSE = \sqrt{\frac{\sum_{i=1}^{n}(y_i - x_i)^2}{n}} \quad (2)$$

3. Results and Discussion

Figure 2 shows the time-series analysis, once per each field, included all VIs computed in all dates. In the graph, the *x*-axis represents the DAS, while the *y*- axis represents the R^2 between VIs and yield in each date. In general, correlations were very low at the very early growth stages because most of the reflected light collected by the satellite comes from soil portions. In Figure 2, correlations were good at the development stages, decreasing at later

stages. This could be explained by the fact that in the more productive parts of the field, the crop grows with high vigour started since the first stages, while in the less productive areas, the crop developed slowly since the beginning. The same trend has been proved in other fields where correlations had a peak at the early stages. Then the curve decreases, probably due to a higher crop uniformity during the higher growth rate stages. In all the seven time-series the trend of the R^2 values was very similar. The highest correlation observed between 80 and 105 DAS. After that the trend usually decreases due to the end of ripening and the following senescing of all green tissues. According to the Italian crops calendar, 80 - 105 DAS coincide with August. In this period, soybean was at the phenological stage R4/R6, it means respectively pods forming, seeds forming, and pods filling. During R4, soybean plants set the number of pods and so the potential productivity. During R5 and R6, soybean metabolism is most focused on grain production and the dry matter increasing has still a positive linear trend. Both in R5 and in R6, most of the dry matter gained and the N storage are due to pods growing and grain forming (Bender et al., 2015). Hence, these are very susceptible stages for soybean development, and any factor of stress in this period could strongly affect the final production (Clay et al. 2013). This could mean soybean health status and chlorophyll content at this range of time is highly related to final production. GCVI, GNDVI, and WDRVI were the highest VIs related to soybean yield and comparing the time-series from all the seven fields. These three indexes explain crops variability better than the others do when vegetation is very dense, the LAI of the canopy is higher than 2 (Gitelson 2004) or LAI is higher than 3 (Viña et al. 2011). This concept is explained in the graph of Figure 3. Figure 3 shows the correlation line between GCVI and NDVI with yield from the field, and date, which shows the highest values. GCVI, which is the best VIs, always maintains a linear trend Figure 3 (a), while NDVI is scattered at higher values Figure 3 (b). Figure 4 illustrates the comparison between the soybean yield map and two VIs maps in the date of maximum correlation. The colours graduation separates lower production areas from higher ones in the same way. In this example, it was easy to understand how strong the relation between the yield variability with VIs maps is. The two fields studied in 2016 show lower correlation values than 2017 and 2018, and the R^2 between GCVI and yield resulted respectively 0.25 and 0.27 in the two fields. Nevertheless, in the two 2016 fields, the highest correlation values are verified at the same DAS range of 80-105, such as in all the other cases. Many answers could explain this issue. There are many constraints that nobody can detect, considering yield maps and satellite images. Many unknown patterns could affect crops production or the light reflected by a crop. For example, severe weather events, pest or disease could damage the crop. GEE filtered the cloudy images above a threshold, but fog or some cirrus could interfere with the actual crop reflected radiation. Moreover, it must be taking into account how the field variability is distributed. Knowing Sentinel-2 observe the average value of a 10 m pixel means large homogeneous zones are easily detected by remote sensing than small and isolated ones. If variability is randomly spread on a field surface, remote sensing could not be the right way to monitor that field. The correlation line between GCVI and the yield has been exploited as the function of the linear model to estimate yield variability. Figure 5 illustrates the actual yield and the predicted yield by the model and the equation used. Table 4 resume the statistical analysis of the products of the linear model, CNS area missed because its GCVI equation was exploited in the model, and the results were already known. The results were good in terms of R^2 and RMSE in the fields cultivated in 2018 and 2017 while the results were not so satisfactory in 2016 fields. First of all, the correlation between yield and VIs was very low this year. It could also mean a linear model could be acceptable to estimate the variability among areas cultivated in the same year but was not accurate enough to do it across the different year. Each year has different weather condition, sowing and harvest date, and any other factor interfering with the correlation between the crop variability and the VIs.

Table 4. RMSE and R^2 values computed between actual yield and predicted yield by the linear model.

	RFS 2018	PVS 2017	AFS 2017	PAS 2017	RZS 2016	BDS 2016
RMSE Mg/ha	0.47	0.61	0.53	0.49	2.07	1.02
R^2	0.49	0.41	0.63	0.52	0.25	0.27

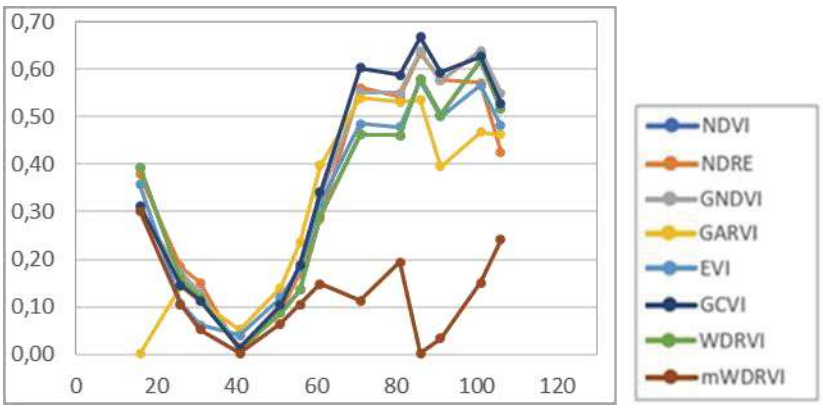

Figure 2. Time-series analysis of the area which showed the higher correlation between soybean yield with eight vegetation indexes computed in all available satellite images. Horizontal axis represents the days after sowing (DAS), while vertical axis means the value of R^2 computed on a different date.

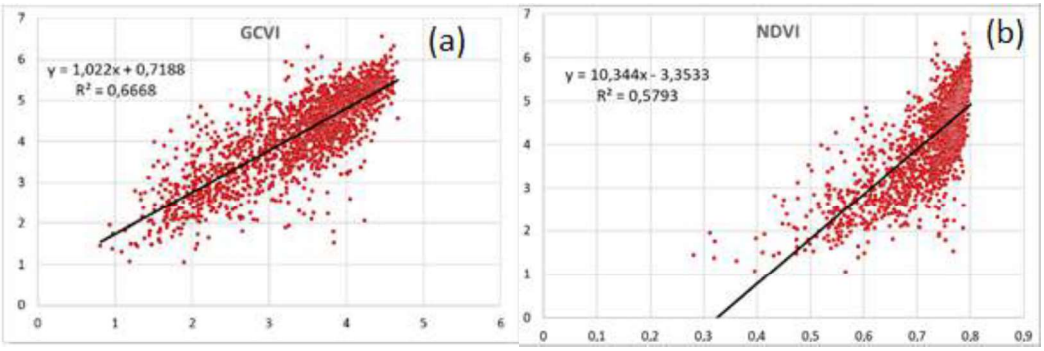

Figure 3. The Scatter plot includes the regression line between GCVI (a) and NDVI (b) values (horizontal axis) and yield (vertical axis). Data comes from the area and the date which showed the highest R^2 value.

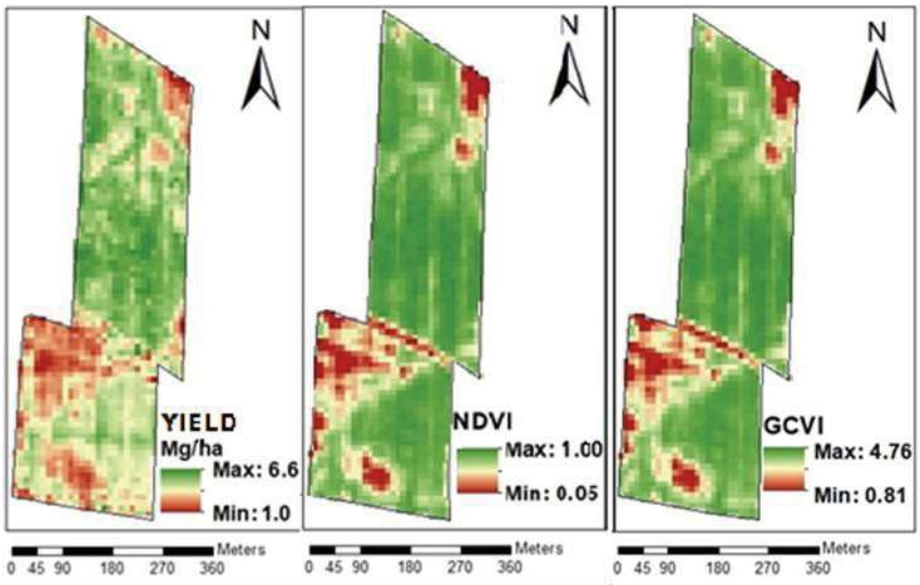

Figure 4. Soybean yield map (10m resolution) from the field with the highest correlation (a), NDVI (b), and GCVI (c) maps of the date with the highest correlation with yield.

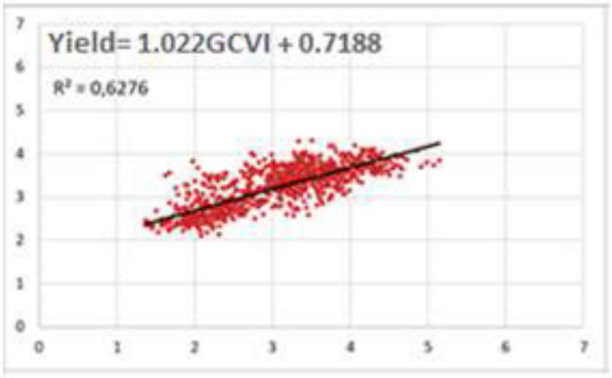

Figure 5. The scatter plot compares the yield predicted by the model on the vertical axis with the actual yield on the horizontal axis; yield is expressed in Mg/ha. (Regression line: yield= 1.022GVI+0.7188)

4. Conclusions

A total of seven yield maps from soybean fields located in North-East of Italy were correlated with eight different VIs derived from Sentinel-2 images. The overall objective was to investigate the ability of Sentinel-2 images to estimate soybean yield variability within-field scale. This research study verified that GCVI, GNDVI, and WDRVI were the best VIs to estimate soybean within-field variability from free Sentinel-2 images. The time-series analysis identified 80 to 105 DAS as the best range of time to detect within-field yield variability from remote sensing. A linear model estimates yield variability in the same area from the VIs raster, but it showed promising results only two years out of three. It suggests a new linear model should be proposed each year to address all the temporal constraints affecting yield and VIs correlation. The use of freely available remote sensing data allows farmers to monitor the within-field variability even though they miss yield maps of their fields or have no other way to monitor their crops. Defining the within-field variability, is essential to all farmers who want to apply precision agriculture: in particular temporal stability of within-field variability can drive farmers decision and support more effective precision farming approaches.

References

Al-Gaadi, Khalid A., Abdalhaleem A. Hassaballa, Elkamil Tola, Ahmed G. Kayad, Rangaswamy Madugundu, Bander Alblewi, and Fahad Assiri. 2016. "Prediction of Potato Crop Yield Using Precision Agriculture Techniques." *PLoS ONE* 11 (9): e0162219. https://doi.org/10.1371/journal.pone.0162219.

Amidan, Brett G., Thomas A. Ferryman, and Scott K. Cooley. 2005. "Data Outlier Detection Using the Chebyshev Theorem." In *IEEE Aerospace Conference Proceedings*. Vol. 2005. https://doi.org/10.1109/AERO.2005.1559688.

Barnes, E M, T R Clarke, S E Richards, P D Colaizzi, J Haberland, M Kostrzewski, P Waller, et al. 2000. "Coincident Detection of Crop Water Stress, Nitrogen Status and Canopy Density Using Ground Based Multispectral Data." *Proc. 5th Int. Conf. Precis Agric*, no. July 2015.

Basso, Bruno, Benjamin Dumont, Davide Cammarano, Andrea Pezzuolo, Francesco Marinello, and Luigi Sartori. 2016. "Environmental and Economic Benefits of Variable Rate Nitrogen Fertilization in a Nitrate Vulnerable Zone." *Science of the Total Environment* 545–546 (March): 227–35. https://doi.org/10.1016/j.scitotenv.2015.12.104.

Bender, R. R.; Haegele, J. W.; Below, F. E. 2015. "Modern Soybean Varieties' Nutrient Uptake Patterns." *Better Crops with Plant Food* 99 (No.2): 7–10.

Bolton, Douglas K., and Mark A. Friedl. 2013. "Forecasting Crop Yield Using Remotely Sensed Vegetation Indices and Crop Phenology Metrics." *Agricultural and Forest Meteorology* 173 (May): 74–84. https://doi.org/10.1016/j.agrformet.2013.01.007.

Clay, David, Charles Carlson, Sharon Clay, Larry Wagner, Darrell Deneke, and Christopher Hay. 2013. "IGrow Soybeans: Best Management Practices for Soybean Production." *Agronomy, Horticulture, and Plant Science Books*, January.

Córdoba, Mariano A., Cecilia I. Bruno, José L. Costa, Nahuel R. Peralta, and Mónica G. Balzarini. 2016. "Protocol for Multivariate Homogeneous Zone Delineation in Precision Agriculture." *Biosystems Engineering* 143 (March): 95–107. https://doi.org/10.1016/j.biosystemseng.2015.12.008.

Foley, William J., Allen McIlwee, Ivan Lawler, Lem Aragones, Andrew P. Woolnough, and Nils Berding. 1998. "Ecological Applications of near Infrared Reflectance Spectroscopy - A Tool for Rapid, Cost-Effective Prediction of the Composition of Plant and Animal Tissues and Aspects of Animal Performance." *Oecologia*. Oecologia. https://doi.org/10.1007/s004420050591.

Gitelson, Anatoly A. 2004. "Wide Dynamic Range Vegetation Index for Remote Quantification of Biophysical Characteristics of Vegetation." *Journal of Plant Physiology* 161 (2): 165–73. https://doi.org/10.1078/0176-1617-01176.

Gitelson, Anatoly A., Yuri Gritz, and Mark N. Merzlyak. 2003. "Relationships between Leaf Chlorophyll Content and Spectral Reflectance and Algorithms for Non-Destructive Chlorophyll Assessment in Higher Plant Leaves." *Journal of Plant Physiology* 160 (3): 271–82. https://doi.org/10.1078/0176-1617-00887.

Gitelson, Anatoly A., Yoram J. Kaufman, and Mark N. Merzlyak. 1996. "Use of a Green Channel in Remote Sensing of Global Vegetation from EOS- MODIS." *Remote Sensing of Environment* 58 (3): 289–98. https://doi.org/10.1016/S0034-4257(96)00072-7.

Huete, A. R. 1988. "A Soil-Adjusted Vegetation Index (SAVI)." *Remote Sensing of Environment* 25 (3): 295–309. https://doi.org/10.1016/0034-4257(88)90106-X.

Hunt, Merryn L., George Alan Blackburn, Luis Carrasco, John W. Redhead, and Clare S. Rowland. 2019. "High Resolution Wheat Yield Mapping Using Sentinel-2." *Remote Sensing of Environment* 233 (November): 111410. https://doi.org/10.1016/j.rse.2019.111410.

James Wilson Rouse, Schell J. A., Donald W. Deering, Robert H. Haas. 1973. "Monitoring Vegetation Systems in the Great Plains with ERTS." In *Proceedings of the Third ERTS Symposium, Goddard Space Flight Center, December 1973, NASA SP-351, NASA, Washington*, edited by NASA, 309–17. Washington: NASA.

Kayad, Ahmed, Marco Sozzi, Simone Gatto, Brett Whelan, Luigi Sartori, and Francesco Marinello. 2021. "Ten Years of Corn Yield Dynamics at Field Scale under Digital Agriculture Solutions: A Case Study from North Italy." *Computers and Electronics in Agriculture* 185 (June). https://doi.org/10.1016/j.compag.2021.106126.

Leroux, Corentin, and Bruno Tisseyre. 2019. "How to Measure and Report Within-Field Variability: A Review of Common Indicators and Their Sensitivity." *Precision Agriculture* 20 (3): 562–90. https://doi.org/10.1007/s11119-018-9598-x.

Liaghat, S., and S. K. Balasundram. 2010. "A Review: The Role of Remote Sensing in Precision Agriculture." *American Journal of Agricultural and Biological Science*. Science Publications. https://doi.org/10.3844/ajabssp.2010.50.55.

Liu, Hui Qing, and Alfredo Huete. 2019. "A Feedback Based Modification of the NDVI to Minimize Canopy Background and Atmospheric Noise." *IEEE Transactions on Geoscience and Remote Sensing* 33 (2): 457–65. https://doi.org/10.1109/tgrs.1995.8746027.

Lobell, David B. 2013. "The Use of Satellite Data for Crop Yield Gap Analysis." *Field Crops Research* 143 (March): 56–64. https://doi.org/10.1016/j.fcr.2012.08.008.

Mahlein, A. K., T. Rumpf, P. Welke, H. W. Dehne, L. Plümer, U. Steiner, and E. C. Oerke. 2013. "Development of Spectral Indices for Detecting and Identifying Plant Diseases." *Remote Sensing of Environment* 128 (January): 21–30. https://doi.org/10.1016/j.rse.2012.09.019.

Oumar, Zakariyyaa, and Onisimo Mutanga. 2013. "Using WorldView-2 Bands and Indices to Predict Bronze Bug (Thaumastocoris Peregrinus) Damage in Plantation Forests." *International Journal of Remote Sensing* 34 (6): 2236–49. https://doi.org/10.1080/01431161.2012.743694.

Sakamoto, Toshihiro, Anatoly A. Gitelson, and Timothy J. Arkebauer. 2013. "MODIS-Based Corn Grain Yield Estimation Model Incorporating Crop Phenology Information." *Remote Sensing of Environment* 131 (April): 215–31. https://doi.org/10.1016/j.rse.2012.12.017.

Schwalbert, Rai A., Telmo J.C. Amado, Luciana Nieto, Sebastian Varela, Geomar M. Corassa, Tiago A.N. Horbe, Charles W. Rice, Nahuel R. Peralta, and Ignacio A. Ciampitti. 2018. "Forecasting Maize Yield at Field Scale Based on High-Resolution Satellite Imagery." *Biosystems Engineering* 171 (July): 179–92. https://doi.org/10.1016/j.biosystemseng.2018.04.020.

Sishodia, Rajendra P., Ram L. Ray, and Sudhir K. Singh. 2020. "Applications of Remote Sensing in Precision Agriculture: A Review." *Remote Sensing* 12 (19): 1–31. https://doi.org/10.3390/rs12193136.

Srbinovska, Mare, Cvetan Gavrovski, Vladimir Dimcev, Aleksandra Krkoleva, and Vesna Borozan. 2015. "Environmental Parameters Monitoring in Precision Agriculture Using Wireless Sensor Networks." *Journal of Cleaner Production* 88 (February): 297–307. https://doi.org/10.1016/j.jclepro.2014.04.036.

Tellaeche, Alberto, Xavier P. BurgosArtizzu, Gonzalo Pajares, Angela Ribeiro, and César Fernández-Quintanilla. 2008. "A New Vision-Based Approach to Differential Spraying in Precision Agriculture." *Computers and Electronics in Agriculture* 60 (2): 144–55. https://doi.org/10.1016/j.compag.2007.07.008.

Thomas, G, J Taylor, and G Wood. 1997. “Mapping Yield Potential with Remote Sensing.”

Thomas Lillesand, Ralph W. Kiefer, Jonathan Chipman. 2015. *Remote Sensing and Image Interpretation, 7th Edition*. Edited by Wiley. 7th ed. New York.

Viña, Andrés, Anatoly A. Gitelson, Anthony L. Nguy-Robertson, and Yi Peng. 2011. “Comparison of Different Vegetation Indices for the Remote Assessment of Green Leaf Area Index of Crops.” *Remote Sensing of Environment* 115 (12): 3468–78. https://doi.org/10.1016/j.rse.2011.08.010.

Xue, Jinru, and Baofeng Su. 2017. “Significant Remote Sensing Vegetation Indices: A Review of Developments and Applications.” *Journal of Sensors*. Hindawi Limited. https://doi.org/10.1155/2017/1353691.

Zhang, Jingcheng, Ruiliang Pu, Wenjiang Huang, Lin Yuan, Juhua Luo, and Jihua Wang. 2012. “Using In-Situ Hyperspectral Data for Detecting and Discriminating Yellow Rust Disease from Nutrient Stresses.” *Field Crops Research* 134 (August): 165–74. https://doi.org/10.1016/j.fcr.2012.05.011.